3. The Pakistan-India outcrop area was on the northern shelf of the Indian Plate, which was close to or straddling the equator at this time; see, for example, A. G. Smith *et al*. [*Atlas of Mesozoic and Cenozoic Coastlines* (Cambridge Univ. Press, Cambridge, 1994)].
4. D. M. Raup and D. Jablonski, *Science* **260**, 971 (1993); D. Jablonski and D. M. Raup, *ibid.* **268**, 389 (1995).
5. Correlation of faunas for the GC: D. T. Dockery III, *Palaios* **1**, 582 (1986); *Miss. Geol*. **17**, 1 (1996); E. A. Mancini and B. H. Tew, *J. Foraminiferal Res*. **21**, 48 (1991); T. G. Gibson and L. M. Bybell, *Soc. Belge Géol. Bull.* **103**, 237 (1994).
6. Correlation of faunas for EU: Special issue on the Northwest European Tertiary Basin, R. Vinken, Ed., *Geol. Jahrb. Reihe A* **100**, 1–508 (1988); J. E. Neal, *Spec. Publ. Geol. Soc. London* **101**, 15 (1996); W. A. Berggren and M.-P. Aubry, *ibid*., p. 309; G. Bignot *et al*., *Neues Jahrb. Geol. Palaeontol. Monatsh*. **1997**, 114 (1997).
7. Correlation of faunas for AF: D. Fournié, *Bull. Centre Rech. Explor.-Prof. Elf-Aquitaine* **2**, 97 (1978); M. F. Megerisi and V. D. Mamgain, *Bull. Dep. Geol. Res. Mining Libya* **12**, 1 (1980); P. Luger, *Berl. Geowiss. Abh*. **A63**, 1 (1985); A. Strougo and A. G. Hewaidy, *Middle East Res. Center Ain Shams Univ. Earth Sci. Ser*. **7**, 190 (1993); A. Strougo, *ibid*. **9**, 1 (1995); A. Kassab *et al*., *Neues Jahrb. Geol. Palaeontol. Abh*. **196**, 309 (1995); M. Faris, *Neues Jahrb. Geol. Palaeontol. Monatsh*. **1997**, 447 (1997).
8. Correlation of faunas for PA: A. Köthe, *Geol. Jahrb. Reihe B* **71**, 3 (1988); A. A. Butt, *Géol. Médit*. **19**, 265 (1992); W. Weiss, *Zitteliana* **20**, 223 (1993).
9. On the basis of the time scale of Berggren *et al*. (*27*). This time scale differs from that used by Hansen *et al*. (*2*), so GC faunal units used here do not coincide exactly with that study. For the Mesozoic time scale used here, see F. M. Gradstein *et al*. [*Soc. Econ. Paleontol. Mineral. Spec. Publ.* **54**, 95 (1995)].
10. Nannofossil zones are grouped into the following intervals: 1, Maastrichtian nannofossil zones upper NC20 to NC23; 2, lower Danian zones NP1 to lower NP3; 3, upper Danian–lower Selandian zones upper NP3 to lower NP4; 4, upper Selandian zones upper NP4 to lower NP5; 5, lower Thanetian zones NP6 to NP8; and 6, upper Thanetian zone NP9. The last Paleocene interval is briefer than the others [1.2 My according to (*27*)], but as this disparity produces no anomalous diversity peaks or valleys, no attempt was made to expand the interval to include the earliest Eocene.
11. T. A. Hansen, *Paleobiology* **14**, 37 (1988).
12. Unfortunately, the regional histories involve pooled composites of museum collections and literature-derived data, so that they generally lack sufficient information for the use of rarefaction analysis based on numbers of specimens or localities [see A. I. Miller and M. Foote, *Paleobiology* **22**, 304 (1996)]. However, provincial faunas are sufficiently large that major differences could only be eliminated by implausible sampling patterns. For example, the next 45 species discovered in EU would all have to belong to the four families identified in the GC as bloom taxa (*11*) for the EU pattern to coincide with the GC one. Furthermore, the bloom taxa tend to be abundant in the GC (*11*), so that sampling biases in faunas elsewhere should enhance their resemblance to the GC rather than decrease it.
13. The interval 2 percentage excursion in AF is not matched in species numbers; indeed, this fauna has the lowest diversity of those studied and thus was probably subject to undersampling biases.
14. W. F. Ponder and A. Warén, *Malacol. Rev. Suppl*. **4**, 288 (1988).
15. J. T. Carlton and J. B. Geller, *Science* **261**, 78 (1993); T. J. Case, *Biol. Conserv*. **78**, 69 (1996).
16. G. J. Vermeij, *Science* **253**, 1099 (1991).
17. The richest interval 2 faunas in EU are from midshelf carbonates, and in AF and PA they are from differing proportions of onshore carbonates and terrigenous sediments; however, the faunal patterns in these three regions are similar, and they contrast with those in the GC [(*5*–*8*); I. Shah, *Mem. Geol. Surv. Pakistan* **12**, 1 (1977); R. Said, Ed., *The Geology of Egypt* (Balkema, Rotterdam, Netherlands, 1990); R. Guiraud, *Geol. Surv. Algeria Mém*. **3**, 1 (1990)]. The GC presents a range of sediment types within interval 2—and subsequent intervals—ranging from offshore claystones in Texas to onshore limestones in Alabama [(*5*); L. D. Toulmin, *Geol. Surv. Alabama Monogr*. **13**, 1 (1977)].
18. N. F. Sohl, *J. Paleontol*. **61**, 1085 (1987).
19. G. Keller, in *Cretaceous-Tertiary Mass Extinctions*, N. MacLeod and G. Keller, Eds. (Norton, New York, 1996), pp. 63–100; C. C. Johnson and E. G. Kauffman, in *ibid*., pp. 231–273. However, in bivalves, high extinction intensities occur in shallow-water carbonate shelves but not in other low-latitude settings (*4*).
20. In contrast, N. MacLeod and G. Keller [*Paleobiology* **20**, 143 (1994)] have suggested that high-latitude regions served as a refuge at the K-T boundary and as a postextinction source for oceanic plankton.
21. P. H. Schultz and S. D'Hondt, *Geology* **24**, 963 (1996).
22. For example, the GC's *Nucula percrassa* lineage is lost at the K-T boundary even though the genus *Nucula* survives to participate in the GC rebound [G. L. Wingard and N. F. Sohl, *U.S. Geol. Surv. Bull*. **1881**, D1 (1991)].
23. For review, see M. E. Power *et al*. [*Bioscience* **46**, 609 (1996)].
24. D. M. Raup, *Science* **206**, 217 (1979).
25. T. J. Case, *Biol. J. Linn. Soc*. **42**, 239 (1991); G. J. Vermeij, *Conserv. Biol*. **78**, 3 (1996); M. H. Williamson and A. Fitter, *ibid*., p. 163; P. B. Moyle and T. Light, *Ecology* **77**, 1666 (1996).
26. P. M. Sheehan and P. J. Coorough [*Mem. Geol. Soc. London* **12**, 181 (1990)] found for the end-Ordovician mass extinction that the high extinction intensities for endemics in North American midcontinent faunas were followed by a similarly unbalanced biotic interchange with European and other faunas.
27. W. A. Berggren *et al*., *Soc. Econ. Paleontol. Mineral. Spec. Publ*. **54**, 129 (1995).
28. D. M. Raup, in *Analytical Paleobiology*, N. L. Gilinsky and P. W. Signor, Eds. (Paleontological Society, Knoxville, TN, 1991), pp. 207–216.
29. J. J. Sepkoski Jr. and D. M. Raup, in *Dynamics of Extinction*, D. K. Elliott, Ed. (Wiley, New York, 1986), pp. 3–36.
30. I thank S. Calzada, R. J. Cleevely, A. V. Dhondt, Y. Edelman, D. H. Erwin, T. A. Hansen, C. Heinberg, C. S. Johnson, E. G. Kauffman, G. L. Kennedy, Z. Lewy, M. Machalski, N. Malchus, L. Marincovich Jr., N. J. Morris, D. B. Rowley, L. R. Saul, F. Schuster, J. J. Sepkoski Jr., A. B. Smith, N. F. Sohl, A. Strougo, J. Todd, T. R. Waller, U. Wielandt, and L. R. Wingard for advice and access to collections or information and S. M. Kidwell and M. Foote for valuable reviews. Supported by NSF grant EAR93-17114; much of this work was done as Research Associate of the Natural History Museum, London.

6 November 1997; accepted 29 January 1998

Geomagnetic Modulation of the ^{36}Cl Flux in the GRIP Ice Core, Greenland

S. Baumgartner, J. Beer,* J. Masarik, G. Wagner, L. Meynadier, H.-A. Synal

Geomagnetic field strength is expected to affect the production rate of cosmogenic isotopes such as beryllium-10, carbon-14, or chlorine-36. Chlorine-36 data from the Greenland Ice Core Project (GRIP) ice core agree well with a production rate calculation based on a paleomagnetic reconstruction for the past 100,000 years over both long- and short-term variations. A chlorine-36 peak at 38,000 years ago previously found in the beryllium-10 record from the Vostok ice core can be explained by a period of low geomagnetic field intensity.

The geomagnetic dipole field shields the Earth from low-energy cosmic ray particles (*1*); this shielding effect is strongest at the magnetic equator and virtually absent at the magnetic poles. Hence, variation of the field strength affects the production rate of cosmogenic isotopes such as ^{14}C, ^{10}Be, or ^{36}Cl. The ^{14}C calibration curve is short, and so a definite interpretation of its long-term variability as a geomagnetic field effect is difficult (*2*). Longer time series, such as a comparison of the Vostok ^{10}Be data with geomagnetic profiles (*3*) and a comparison of geomagnetic paleointensity and ^{10}Be in the same core (*4*), support the correlation for the past 100,000 years, but it has been difficult to demonstrate a correlation on short time scales. Here, we present a high-resolution investigation into the correlation between a radioisotope flux curve and a geomagnetic field reconstruction using data from the GRIP ice core.

The abundance of ^{36}Cl and ^{10}Be for the past 100,000 years has been measured in the Summit GRIP ice core (*5*, *6*). Similar data are available in the Summit Greenland Ice Sheet Project 2 (GISP2) ice core (*7*), but at a somewhat lower resolution. We assume that the flux of ^{36}Cl and ^{10}Be over southern and central Greenland is directly related to the global average production of these isotopes. Greenland receives a considerable part of its precipitation from lower latitudes, and this pattern persisted during the last ice age (*8*). Therefore, it is unlikely that the flux of ^{36}Cl and ^{10}Be is dominated by local radioisotope production, which is not very

S. Baumgartner, J. Beer, J. Masarik, G. Wagner, Environmental Physics, Swiss Federal Institute of Science and Technology, CH-8600 Dübendorf, Switzerland.
L. Meynadier, Laboratoire de Geochimie et Cosmochimie, CNRS 1758, Institut de Physique du Globe de Paris, 4 place Jussieu, F-75252 Paris Cedex 5, France.
H.-A. Synal, Paul Scherrer Institut, c/o Eidgenössische Technische Hochschule Hönggerberg, CH-8093 Zürich, Switzerland.

*To whom correspondence should be addressed.

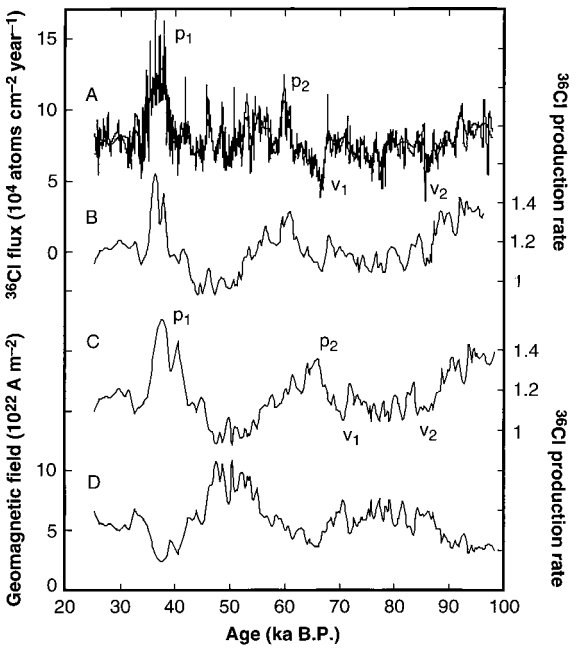

Fig. 1. (**A**) ^{36}Cl flux as calculated from the measured ^{36}Cl concentrations in the GRIP ice core from Summit, Greenland: raw data (thin curve) and low-pass filtered data (cutoff frequency = 1/2000 years; thick curve). (**B**) Geomagnetically controlled ^{36}Cl production rate shifted in time to match the major wiggles in (A). (**C**) Geomagnetically controlled ^{36}Cl production rate on its own time scale, calculated from the data shown in (D). (**D**) Geomagnetic field intensity (virtual axial dipole moment) as reconstructed from three sediment cores from the Somali Basin (*15*).

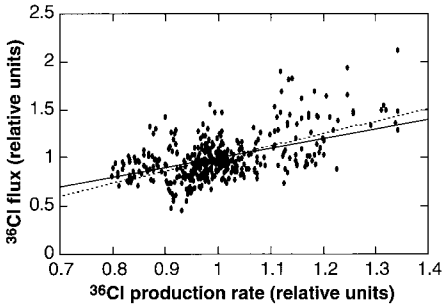

Fig. 2. ^{36}Cl flux from Summit (raw data from Fig. 1A) as a function of ^{36}Cl production rate (data from Fig. 1B). Both data sets are averaged to unity. Expected (solid line) and real (dashed line) correlation between both data sets.

sensitive to geomagnetic modulation. Any variability of the geomagnetic dipole field strength therefore should be reflected in the radioisotope flux over Greenland.

At present, 406 ^{36}Cl samples have been measured in the depth interval between 2000 and 2700 m of the Summit GRIP ice core, which corresponds to the period of 25 to 96 thousand years ago (ka) (*9*); the data have been calibrated with University of California, San Diego, standard material (NBS SRM4422L) (*10*). Measurement uncertainties are calculated with the 1σ error introduced from the counting statistics and uncertainties from normalization and background correction. The mean error of all measured samples is 7%. The sample density corresponds to a mean time resolution of 200 years, which is higher at the end of the last ice age (~100 years) than at its beginning (~300 years).

The measured ^{36}Cl concentrations of the ice have been corrected for radioactive decay (half-life = 301 ka) (*11*). The maximum correction is 26% at 100 ka. The excellent δ^{18}O correspondence between the GRIP and GISP2 ice cores to a depth of 2750 m (*12*), corresponding to an age of about 90 ka for the GRIP core (*9*), indicates that both records are essentially undisturbed down to this depth. The ^{36}Cl records correlate well also (*5*, *7*). The time scales for the two cores from Summit differ by several thousand years, however (*13*). Because the Younger Dryas at 11.5 ka and the Eem transition at 110 ka are well dated elsewhere, we assume that the error of the GRIP time scale used does not exceed 10%. This assumption leads to a maximum error of 3% in the ^{36}Cl concentrations because of the age correction, which is considerably smaller than the ^{36}Cl measurement uncertainties.

The ^{36}Cl signal in ice is basically composed of two components: production and transport. To remove the transport component, we calculated the ^{36}Cl flux by multiplying the measured ^{36}Cl concentrations by the accumulation rate and the density of ice (Fig. 1A). The accumulation rate was estimated on the basis of the relation between δ^{18}O and the annual layer thickness (*9*). The resulting ^{36}Cl flux is independent of the basic climate proxy δ^{18}O (*5*).

Several recent reconstructions of the geomagnetic field strength (*14*–*17*) of the past 100 ka derived from measurements of the magnetic remanence in sediment cores have yielded fairly consistent results (*18*). For specific comparison, we used a reconstruction of the geomagnetic field intensity based on three sediment cores drilled in the Somali Basin, located east of Africa (*15*). This record was chosen instead of others (*14*–*18*) because of its high temporal resolution. Other comparable paleomagnetic studies show a good correlation even in the fine structure (*14*, *16*). The Somali Basin record agrees well with the synthetic Sint-200 stack, which was constructed from 18 independent paleomagnetic records (*18*).

On the basis of the Somali Basin record, we calculated global ^{36}Cl production rates using a model that predicts a nonlinear polynomial increase in ^{36}Cl production for decreasing geomagnetic dipole field intensity (*19*). To simulate the effect of a change in geomagnetic field intensity, we varied the latter from 0 to 2 times the present value before calculating the particle fluxes and nuclide production in the Earth's atmosphere. The obtained dependence for the global average ^{36}Cl production rate can be described by a fifth-degree polynomial (*19*). Compared with present field strength and mean present solar activity, ^{36}Cl production is enhanced by a factor of 2.1 for a zero magnetic dipole field.

Overall, the measured ^{36}Cl flux (Fig. 1A) agrees well with the calculated production rate (Fig. 1C). The most prominent features are peaks (p_1 and p_2) at about 38 and 60 ka and lows (v_1 and v_2) at about 70 and 85 ka. There is some similarity in the fine structure, for example, in the number of peaks around 60 ka (subpeaks of p_2) or around 80 ka. The peak (p_1) at 38 ka was discovered in the ^{10}Be record of the Vostok ice core (*20*) and subsequently identified in other ice (*21*) and sediment (*22*) cores. It has been attributed to a period of low geomagnetic field (*3*), a period of low solar activity, or a supernova explosion (*23*). In contrast, the enhancement in the field strength at about 50 ka is not seen in the ^{36}Cl flux.

The qualitative agreement of these two totally independent curves encouraged us to construct a common time scale of both records by a wiggle-matching procedure. Because the maximum difference of 5500 years at about 60 ka is still within the uncertainties of the two original time scales (*13*, *15*), we shifted—rather arbitrarily—the magnetic record to match the GRIP time scale (Fig. 1B). Using the new time scale, we interpolated the ^{36}Cl production rate data to the raw ^{36}Cl flux data by use of a cubic spline. Both data sets were averaged to unity for the period 25 to 95 ka. Although the scatter is large, a correlation between both data sets is visible (Fig. 2).

If all underlying assumptions are correct and if measured and calculated amplitudes agree, one would expect a linear correlation with a slope of 1.00 and an intercept of 0.00 (solid line in Fig. 2); the actual slope is

1.21 ± 0.09 (1 σ) and the intercept is –0.21 ± 0.09 (1 σ) (dashed line in Fig. 2). Thus, our model explains about 100% of the ^{36}Cl flux variability, which is in covariance with the magnetic variability. It is rather difficult, however, to interpret the calculated parameter errors in terms of confidence intervals because of the fitted time scale.

The correlation of $r = 0.56$ ($n = 406$) between the unfiltered ^{36}Cl flux and the calculated production rate data indicates that about 30% of the total variance of the unfiltered ^{36}Cl flux can be explained by geomagnetically induced production variations. For low-pass filtered data (frequency = 1/3000 years), the correlation rises to $r = 0.67$. The remaining variance is larger than the experimental errors and therefore still contains information about other paleoenvironmental factors. Changing climatical and meteorological conditions may alter transport, deposition, and concentration of ^{36}Cl in ice. The sedimentation process may affect the record of magnetic intensity; short-time geomagnetic variability cannot be monitored yet by corresponding archives. Cosmic ray intensity as well as solar activity fluctuations have to be taken into account, too.

Thus, our study agrees well with an investigation that attributes the 38-ka ^{10}Be peak in Antarctica to a low value of the geomagnetic field (*3*). This agreement indicates long-range transport of ^{10}Be from lower latitudes to Antarctica during the last glacial. Beryllium-10 studies in Holocene ice reveal a strong local production component in Antarctica (*24*), however. Although not yet conclusive, these results point to a change in the transport pattern of the Southern Hemisphere between the last glacial period and the Holocene.

Our observations support the reliability of marine sediments as recorders of geomagnetic intensity variations; they also provide an independent approach to reconstruct the history of the geomagnetic dipole field.

REFERENCES AND NOTES

1. D. Lal and B. Peters, in *Handbuch der Physik* (Springer-Verlag, Heidelberg, Germany, 1967), vol. 46, pp. 551–612.
2. J. Beer *et al*., *Nature* **331**, 675 (1988).
3. A. Mazaud, C. Laj, M. Bender, *Geophys. Res. Lett.* **21**, 337 (1994).
4. C. Robinson, G. M. Raisbeck, F. Yiou, B. Lehman, C. Laj, *Earth Planet. Sci. Lett.* **136**, 551 (1995).
5. S. Baumgartner *et al*., *J. Geophys. Res.* **102**, 26659 (1997).
6. F. Yiou *et al*., *ibid.*, p. 26783.
7. R. C. Finkel and K. Nishiizumi, *ibid.*, p. 26699.
8. S. J. Johnsen, W. Dansgaard, J. W. C. White, *Tellus Ser. B* **41**, 452 (1989); C. D. Charles, D. Rind, J. Jouzel, R. D. Koster, R. G. Fairbanks, *Science* **263**, 508 (1994).
9. W. Dansgaard *et al*., *Nature* **364**, 218 (1993).
10. P. Sharma *et al*., in *5th International Conference on AMS*, Paris, 23 to 27 October 1990, F. Yiou and G. M. Raisbeck, Eds. (North-Holland, Amsterdam, 1990), pp. 410–415.
11. H. W. Bentley, F. M. Phillips, S. N. Davis, in *Handbook of Environmental Isotope Geochemistry,* P. Fritz and J. C. Fontes, Eds. (Elsevier, Amsterdam, 1986), vol. 2, pp. 427–480.
12. P. M. Grootes, M. Stuiver, J. W. C. White, S. Johnsen, J. Jouzel, *Nature* **366**, 552 (1993).
13. C. U. Hammer and D. A. Meese, *ibid.* **363**, 666 (1993); M. Bender *et al*., *ibid.* **372**, 663 (1994).
14. E. Tric *et al*., *J. Geophys. Res.* **97**, 9337 (1992).
15. L. Meynadier, J. P. Valet, R. Weeks, N. J. Shackleton, V. L. Hagee, *Earth Planet. Sci. Lett.* **114**, 39 (1992).
16. J. S. Stoner, J. E. T. Channell, C. Hillaire-Marcel, *ibid.* **134**, 237 (1995).
17. D. A. Schneider, *ibid.* **120**, 301 (1993); B. Lehman *et al*., *Phys. Earth Planet. Inter.* **93**, 269 (1996); D. V. Kent and N. D. Opdyke, *Nature* **266**, 156 (1977); T. Yamazakia, N. Ioka, N. Eguchi, *Earth Planet. Sci. Lett.* **136**, 525 (1995).
18. Y. Guyodo and J.-P. Valet, *ibid.* **143**, 23 (1996).
19. J. Masarik and J. Beer, in *Proceedings of the 25th International Cosmic Ray Conference*, Space Research Unit, Potchefstroom University, Durban, South Africa, 30 July to 6 August 1997 (Potchefstroom University, Durban, South Africa, 1997), vol. 2, pp. 461–464. In our code, the incident primary cosmic ray particles are transported through the matter considering ionization energy losses and nuclear elastic and inelastic scattering. This code uses only basic physical quantities and parameters, without any free parameters, to numerically simulate all processes relevant in particle production and transport. It enables us to trace the fate of each individual particle and in doing so to study in detail the effects of various parameters on production rates, including geomagnetic field variations. For long-term average solar activity, the dependence of the ^{36}Cl production rate P on the geomagnetic field intensity B can be approximated by the polynomial: $P = 2.11 - 2.81B + 3.17B^2 - 2.09B^3 + 0.73B^4 - 0.10B^5$ (P and B are relative to their present value). The polynomial coefficients are dependent on solar activity and differ slightly for particular isotopes. For weak geomagnetic fields, our model gives production rates that are 15% higher than those from the widely used model of Lal and Peters (*1*).
20. G. M. Raisbeck *et al*., *Nature* **326**, 273 (1987).
21. J. Beer *et al*., in *The Last Deglaciation: Absolute and Radiocarbon Chronologies,* E. Bard and W. S. Broecker, Eds. (Springer-Verlag, Berlin, 1992), vol. 12, pp. 141–153.
22. G. C. Castagnoli *et al*., *Geophys. Res. Lett.* **22**, 707 (1995); L. R. McHargue, P. E. Damon, D. J. Donahue, *ibid.*, p. 659.
23. C. P. Sonett, *Radiocarbon* **34**, 239 (1992).
24. E. Bard, G. M. Raisbeck, F. Yiou, J. Jouzel, *Earth Planet. Sci. Lett.* **150**, 453 (1997); E. J. Steig, P. J. Polissar, M. Stuiver, P. M. Grootes, R. C. Finkel, *Geophys. Res. Lett.* **23**, 523 (1996).

25. We thank the technical staff of the Swiss Federal Institute of Science and Technology, the accelerator group at the Paul Scherrer Institut–Eidgenössische Technische Hochschule accelerator mass spectrometry facility, and the GRIP field team for their help and S. Johnsen for transmitting the δ^{18}O data from the Summit GRIP ice core. Supported by the Swiss National Science Foundation.

16 October 1997; accepted 21 January 1998

Carbonic Acid in the Gas Phase and Its Astrophysical Relevance

Wolfgang Hage, Klaus R. Liedl,* Andreas Hallbrucker, Erwin Mayer*

In outer space, high-energy irradiation of cryogenic ice mixtures of abundant water and carbon dioxide is expected to form solid carbonic acid. Experiments and thermodynamic analyses show that crystalline carbonic acid sublimates without decomposition. Free-energy considerations based on highly accurate molecular quantum mechanics, in combination with vapor pressures resulting from experimental sublimation rates, suggest that in the gas phase, a monomer and dimer of carbonic acid are in equilibrium, comparable to that of formic acid. Gaseous carbonic acid could be present in comets, on Mars and outer solar system bodies, in interstellar icy grains, and in Earth's upper atmosphere.

Carbonic acid (H_2CO_3), the short-lived intermediate in CO_2-HCO_3^-/CO_3^{2-} proton transfer reactions, is a key compound in biological and geochemical carbonate-containing systems (*1*–*5*). At ambient temperature, H_2CO_3 dissolved in water dissociates rapidly into CO_2 and H_2O, with a rate constant of ~20 s^{-1} and an activation enthalpy of ~70 kJ mol^{-1}; the reaction is highly exergonic (*1*–*5*). Carbonic acid has recently been synthesized at low temperatures by two basically different routes: (i) high-energy irradiation of cryogenic CO_2/H_2O ice mixtures (*6*–*9*) and proton-irradiation of pure solid CO_2 (*9*), and (ii) protonation of bicarbonate or carbonate in a new cryogenic technique (*10*–*14*). Fourier-transform infrared spectroscopic studies led to characterization of two polymorphs. One (β-H_2CO_3) is formed by high-energy irradiation (*6*–*9*) or by protonation in freeze-concentrated aqueous solution (*11*, *13*, *14*). The other (α-H_2CO_3) is formed by protonation in methanolic solution (*10*–*12*, *14*), with β-H_2CO_3 transforming into α-H_2CO_3 (*11*). For the gas phase of H_2CO_3, high-level molecular quantum mechanical calcu-

Institut für Allgemeine, Anorganische und Theoretische Chemie, Universität Innsbruck, A-6020 Innsbruck, Austria.

*To whom correspondence should be addressed. E-mail: klaus.liedl@vibk.ac.at and erwin.mayer@uibk.ac.at